A marsupial robotic fish team: Design, motion and cooperation

Chao ZHOU, ZhiQiang CAO, Shuo WANG and Min TAN

Citation: SCIENCE CHINA Technological Sciences **53**, 2896 (2010); doi: 10.1007/s11431-010-4145-7

View online: http://engine.scichina.com/doi/10.1007/s11431-010-4145-7

View Table of Contents: http://engine.scichina.com/publisher/scp/journal/SCTS/53/11

Published by the Science China Press

SCIENCE CHINA
Technological Sciences

November 2010 Vol.53 No.11: 2896–2904
doi: 10.1007/s11431-010-4145-7

A marsupial robotic fish team: Design, motion and cooperation

ZHOU Chao*, CAO ZhiQiang, WANG Shuo & TAN Min

Laboratory of Complex Systems and Intelligence Science, Institute of Automation, Chinese Academy of Sciences, Beijing 100190, China

Received May 6, 2010; accepted August 28, 2010

A bio-inspired marsupial robotic fish system composed of heterogeneous robotic fish is proposed in this paper. A miniature robotic fish, as the daughter robotic fish, can adapt to some narrow space, while the mother robotic fish, with a cabin to transport the daughter, possesses a powerful movement ability to improve the mobility and endurance of the team. The structures for mimicking bio-motion and the method for fishlike-motion are presented. A typical task of daughter-mother following is given to show the cooperation of the team. A motion model of free swimming is built based on the Lagrangian function, and the coupled dynamic and kinematic functions are calculated based on the relation between the generalized force and fluid force. Then, a neural network is trained through the data generated from this model to get a predictive yaw controller, which can control the orientation by a different offset of each link. The daughter robotic fish adopts a dynamic light source tracking approach to follow the mother, and a heterogeneous communication-based finite state machine is presented for task modeling. Experiments are carried out to verify the system.

marsupial robotic fish, daughter-mother following, heterogeneous communication-based FSM

Citation: Zhou C, Cao Z Q, Wang S, et al. A marsupial robotic fish team: Design, motion and cooperation. Sci China Tech Sci, 2010, 53: 2896–2904, doi: 10.1007/s11431-010-4145-7

1 Introduction

Investigation on biomimetic systems has provided significant insights into both theory and application of robotics in recent years. Under the category of biology-inspired swimming robots, robotic fish has received much attention, whose appealing nature involves higher efficiency, more remarkable maneuverability, and quieter actuation than conventional underwater vehicles equipped with thrusters [1–3]. These advantages are of great benefit to applications in marine and military fields such as underwater operation, military reconnaissance, leakage detection, etc. Biomimetic robotic fish is generally defined as a fish-like aquatic vehicle based on the swimming skills and anatomic structure of a fish: the undulatory/oscillatory body motions, the highly controllable fins and the large aspect ratio lunate tail.

As a new idea to explore secrets of the fish's prominent swimming skill, many biomimetic robotic fish prototypes have been developed. MIT had successfully developed an eight-link, fish-like swimming machine called RoboTuna [1]. RoboTuna and subsequent RoboPike [4] projects attempted to create AUVs with increasing energy savings and longer mission duration by utilizing a flexible posterior body and a flapping foil (tail fin) that exploited external fluid forces to produce thrust. Kato has considered the control of pectoral fins-like mechanical structure as a propulsor and built a Blackbass Robot [5] and a BASS-II [6]. In Nagoya University, Fukuda developed a fish-like micro robot, which possessed a pair of fins actuated by piezoceramics [7]. The G series and MT series robotic fishes have been developed by the University of Essex [8]. The undulating robotic fish developed by Low is a ribbon fin type robotic fish [9]. Institute of Automation, Chinese Academy of Sciences has

*Corresponding author (email: zhouchao@compsys.ia.ac.cn)

been studying the control and coordination of robotic fish [10, 11].

Inspired by marsupial animals, e.g. kangaroo, and the related works, e.g. marsupial and shape-shifting robots for urban search and rescue [12, 13], a heterogeneous marsupial robotic fish system is proposed for the purpose of resolving contradictions of applications in this paper. The robotic fish are expected to work in unreachable places for human being, such as the gap of rock, the inside of oil pipeline and the interior of sunken ship. The development of miniature robotic fish with high maneuverability and adaptability is of great advantages. On the other hand, the miniature robotic fish is convenient enough to be mass-produced, which may enhance the overall performance by cooperation among them. Although miniaturization of the robotic fish is useful in some situations, the limited volume restricts the capability. The team in this study is composed of a mother robotic fish (MRF) with a cabin for a miniature robotic fish, as a daughter robotic fish (DRF). MRF can carry DRF and move together to the designated workplace, release DRF and assist it with the task. In this heterogeneous team, MRF can swim for long endurance, and has a strong ability of movement and may be mounted more sensors, which compensate shortages of the miniaturization of DRF.

The yaw control of the system is described in detail. The yaw control of robotic fish needs to calculate the offset of each link in every control cycle. However, the effect of the orientation variation is hard to control due to the complicated force. A model for free swimming without the assumption of non-oscillatory head motion is required for the yaw control, and a neural network predictive controller, which is trained via the model, is proposed to calculate the deflection of each link to control the turning motion.

A specific issue related to the daughter-mother following task is addressed to show the cooperation of the team. The sensor-based dynamic light source tracking approach for DRF is proposed to follow the mother and a heterogeneous communication-based finite state machine (HCFSM) is given to model the task of cooperation. As a new concept of robotic fish prototype, the marsupial team may be used potentially in many situations.

2 The robotic fish prototype

2.1 MRF and basic bio-motions

The mother robotic fish is expected to transport DRF. The Carangiform mode [14] is chosen as the natural prototype, as shown in Figure 1. Four links swing with the caudal fin to propel the robotic fish forward like the spine and tail of fish. The control module, the communication module, the battery and other devices are installed inside the head. A cabin on MRF is used to carry DRF. The cabin can open and release the DRF. The controllable light source on MRF provides a good media for establishing the connection between MRF and DRF. The body-tail undulation is assumed to be a traveling wave, which travels from the head to the tail, gradually increasing amplitude [8, 11]. The propulsive system is controlled based on the swimming gaits to generate propulsion, and the speed can be adjusted by the frequency and amplitude of the body-tail undulation, or the length of the body-tail undulatory part.

The method of changing the barycenter [10] is selected to implement three-dimensional locomotion of MRF. As shown in Figure 1, the servo motor of the barycenter-adjustor rotates to adjust the position of the weight, and the centre of gravity of the robotic fish changes simultaneously. With the balance of the gravity moment and the buoyancy moment, the pitching angle of the robotic fish can be adjusted, and the posture change can be done too. When the weight is in the middle position, the robotic fish keeps horizontal and the pitching angle is zero. When the weight moves forward or backward, the robotic fish will pitch down or up. The rotation speed of the adjustor's servo should be fast compared to the movement of the fish robot, and the weight of the adjustor should be heavy enough to make the pitching posture sensitive to change of the adjustor's position. A pressure sensor can measure the water

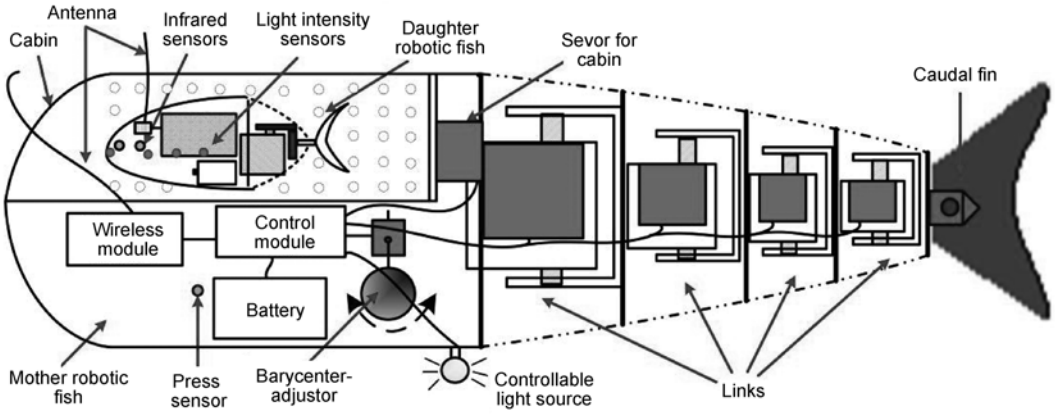

Figure 1 Schematic diagram of the experiment platform.

pressure as a feedback to the depth control [10].

2.2 DRF and basic bio-motions

DRF is a Thunniform-mode-based miniature robotic fish, as shown in Figure 1. Thunniform mode is one of the most efficient modes, where thrust is generated with a lift-based method [14]. Significant lateral movements occur only at the caudal fin. In addition, the reduction of the length of the undulating part will simplify the structure and reduce the volume on the whole.

A servo motor is adopted to drive a lunate caudal fin as the thruster of the robotic fish, according to fish outline and its motion characteristics [11]. All assembly units are highly cost-effective because of volume restriction. The controller integrates the functions of information acquisition and processing, communication, motion decision and control. Besides infrared sensors, light density sensors are mounted to detect the light source, which is carried by MRF.

MRF and DRF may cooperate with each other to accomplish the assigned task. The wireless communication is adopted between the upper console and MRF and DRF. MRF and DRF may cooperate with each other to accomplish the task assigned by the upper console. In addition, MRF may be the information relay between DRF and the upper console.

2.3 The system integration

In many missions, cooperations of robotic fish pay more attention on the yaw control, which works on the track of the robotic fish. However, the yaw control is very difficult due to the complicated swimming mechanism. In order to deal with this problem, a motion model is built to train a neural network controller as to calculate the deflection of the robotic fish joints, and a decision making method is given to compute the direction of advance according to the multiple sources of sensor information. A cooperation mechanism is developed to model the mission, and to generate the relative motion of MRF and DRF based on the NN yaw controller and the decision making method. The control diagram is shown in Figure 2.

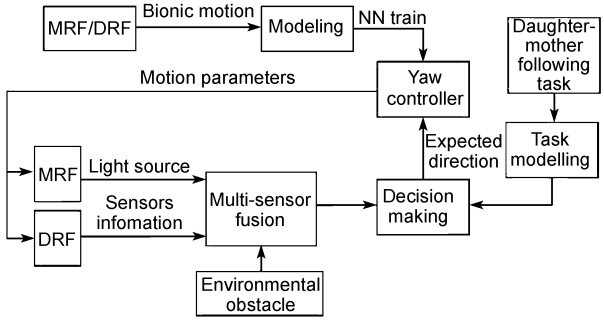

Figure 2 The control diagram of the system.

3 Yaw control of the robotic fish

The yaw control is the most important part in motion of cooperation. However, the yaw control method of robotic fish is still lacking of extensive study. In the previous work, the head undulation (the first link) of robotic fish was ignored [15, 16] because its amplitude was very small compared with the propulsion. However, this assumption is not suitable in yaw control. The oscillatory action of the head is very important for changing the orientation. Thus, a model for free swimming without the assumption of non-oscillatory head motion is required. On the other hand, the propulsion direction of the robotic fish can be controlled by changing the symmetric center of undulation, which means the yaw control must calculate the offset of each link in every control cycle. However, the effect of the orientation variation is hard to control due to the complicated force. In this paper, a neural network predictive controller, which is trained via the model, is proposed to calculate the deflection of each link to control the turning motion.

3.1 The model of multi-link undulation

While swimming in water, the robotic fish pushes water away and backward with undulation of the tail fin and the body, and then gets propelled. The carangiform robotic fish considered in this paper consists of three parts: a stiff anterior body, a flexible rear body, and an oscillating lunate caudal fin. The whole body of the fish, from a mechanical engineering perspective, can be designed as a multi-link mechanical structure, consisting of several oscillating hinge joints actuated by motors. This structure is a typical serial structure, and MRF in Figure 1 gives an example of five links, and DRF is of two links.

The swimming gaits for the multi-link structure are calculated by the following method. Assume the fish has N links, $l_1, \cdots, l_N$, and the angle of joint ϕ_i is [11]

$$\varphi_i(j) = A_i \sin(2\pi / M \cdot j + \psi_i) + \delta_i, \quad (1)$$

where φ_i is the angle between l_i and l_{i+1}. A_i is the amplitude of the ith joint angle, and ψ_i is the phase, i=1, $\cdots$, N–1. δ_i is the deflection on the ith link, and all δ_i are usually equal in applications. N=5 in MRF and N=2 in DRF.

The robotic fish may be considered as a typical serial robot, and it can be described by the Lagrangian function. However, one significant difference between them is that the motion of the robotic fish has neither any fixed points (e.g. the base frame of a mechanical arm), nor any fixed reference systems (e.g. the ground reference frame of a mobile robot). The robotic fish swims in water freely, and the motion of its links interacts with the water: the motion determines the magnitude and direction of the hydrodynamic force, which reversely determines the fish's movement. The kinematic and dynamic problems are thus coupled, and can

not be calculated individually. Eq. (1) gives the relative motion laws of the links.

The basic idea for modeling the biomimetic robotic fish is to build the Lagrangian function. The generalized forces obtained from the Lagrange equation of the second kind are equal to the force calculated by the hydrodynamics. Finally, a system of partial differential equations can be built. Some assumptions are given to simplify the modeling:

A1. The body of the robotic fish can be considered as N jointed plates [17].

A2. The robotic fish swims in still water, and it is not affected by reflected waves in the environment.

A3. The deformation of the robotic fish can be ignored except the motion of the joints.

A4. The motion is analyzed only in two dimensions, which is the most important propulsion situation.

The top view of the simplified multi-link structure is shown in Figure 3, where parameters are labeled with respect to XOY, the world rectangular coordinate system (WRCS).

In Figure 3, l_i is the ith link of the robotic fish, and also the length of the link. θ_i is the angle between ith link and polar axis. φ_i is the angle between ith link and extension line of $(i-1)$th link. The parameters θ_i and φ_i are both anti-clockwise positive. $(x_i^{\mathrm{f}}, y_i^{\mathrm{f}})$, $(x_i^{\mathrm{g}}, y_i^{\mathrm{g}})$ and (x_i, y_i) are the center of figure, the center of gravity and the beginning point of ith link, respectively. The joint angle φ_i is known by eq. (1).

The potential energy is constant E_{p} according to the assumption A4. The kinetic energy of each link consists of the translational part with respect to the WRCS and the rotational part with respect to the centre-of-mass system. Thus, the Lagrangian function is defined as follows:

$$\begin{aligned} L &= \sum_{i=1}^{N}\frac{1}{2}m_i v_i^2 + \sum_{i=1}^{N}\frac{1}{2}I_i\omega_i^2 - E_{\mathrm{p}} \\ &= \sum_{i=1}^{N}\frac{1}{2}m_i\left(\left(\dot{x}_i^{\mathrm{g}}\right)^2 + \left(\dot{y}_i^{\mathrm{g}}\right)^2\right) + \sum_{i=1}^{N}\frac{1}{2}I_i\left(\dot{\theta}_i\right)^2 - E_{\mathrm{p}}, \end{aligned} \tag{2}$$

where m_i is the mass and the added mass of the ith link. I_i is the moment of inertia of the ith link with respect to the centre-of-mass system.

Then, x_1, y_1, θ_1 are selected as the generalized coordinates, namely $X = x_1$, $Y = y_1$, $\Theta = \theta_2$. Rewrite the Lagrangian function $L = L(X, Y, \Theta)$ as follows

$$\begin{aligned} L = {} & \frac{1}{2}m_1\left(\dot{X} + (l_1 - l_1^{\mathrm{g}})\left(\dot{\Theta} - \dot{\varphi}\right)\sin\left(\Theta - \varphi\right)\right)^2 \\ & + \frac{1}{2}m_2\left(\dot{X} + l_2^{\mathrm{g}}\dot{\Theta}\sin\Theta\right)^2 + \frac{1}{2}I_1\left(\dot{\Theta} - \dot{\varphi}\right)^2 \\ & + \frac{1}{2}m_1\left(\dot{Y} - \left(l_1 - l_1^{\mathrm{g}}\right)\left(\dot{\Theta} - \dot{\varphi}\right)\cos\left(\Theta - \varphi\right)\right)^2 \\ & + \frac{1}{2}m_2\left(Y - l_2^{\mathrm{g}}\dot{\Theta}\cos\Theta\right)^2 + \frac{1}{2}I_2\dot{\Theta}^2 \\ & + \sum_{i=3}^{N}\frac{1}{2}m_i\left[\frac{\mathrm{d}}{\mathrm{d}t}\left(X + \sum_{j=2}^{i-1}l_j\cos\theta_j + l_i^{\mathrm{g}}\cos\theta_i\right)\right]^2 \\ & + \sum_{i=3}^{N}\frac{1}{2}m_i\left[\frac{\mathrm{d}}{\mathrm{d}t}\left(Y + \sum_{j=2}^{i-1}l_j\sin\theta_j + l_i^{\mathrm{g}}\sin\theta_i\right)\right]^2 \\ & + \sum_{i=3}^{N}\frac{1}{2}I_i\left[\frac{\mathrm{d}}{\mathrm{d}t}\left(\Theta + \sum_{j=2}^{N-1}\varphi_j\right)\right]^2 - E_{\mathrm{p}}, \end{aligned} \tag{3}$$

where l_i^{g} is the distance between $(x_i^{\mathrm{g}}, y_i^{\mathrm{g}})$ and (x_i, y_i).

The hydrodynamic forces acting on the robotic fish are determined by the instantaneous movement. A hydrodynamic drag model that has been extensively used in the literature in the case of large Reynolds numbers [16, 18] is employed to analyze the forces perpendicular to the surface of the swimming robotic fish. The hydrodynamic force then is

$$F = -\mu\,\mathrm{sgn}(v^{\perp})(v^{\perp})^2, \tag{4}$$

where $\mu = \rho CS/2$ is the drag coefficient. ρ, C and S are the density of water, the shape coefficient and the effective area, respectively. $v^{\perp}$ is the projection of the velocity along the direction perpendicular to the surface.

The force acting on the robotic fish is divided into two parts: pressure on the links and approach stream pressure. The first part denotes the hydrodynamic force on the robotic

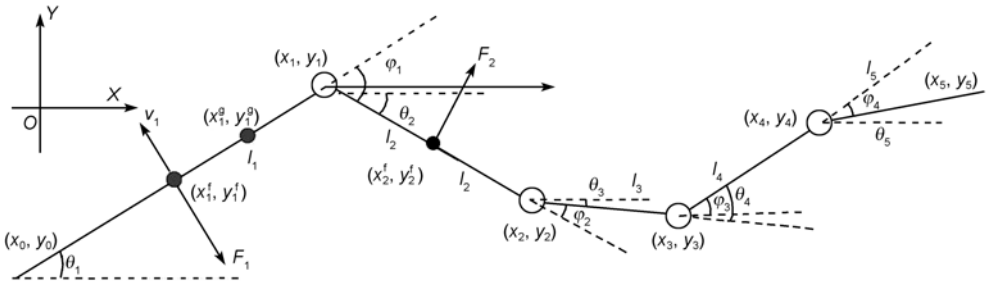

Figure 3 The simplified robotic fish and definition of parameters.

fish's ith link when it swings:

$$F_i^{\perp} = -\mu^{\perp} \operatorname{sgn}(v_i^{\perp}) \left| v_i^{\perp} \right|^2, \tag{5}$$

where $F_i^{\perp}$ is the pressure on ith link, $v_i^{\perp}$ is the projection of the velocity of *i*th link along the perpendicular direction, and $\mu^{\perp}$ is the drag coefficient.

The approach stream pressure is introduced because the water pushes on the cross section of the robotic fish when the robotic fish advances:

$$F_1^{=} = -\mu^{=} \operatorname{sgn}(v_1^{=}) \left| v_1^{=} \right|^2, \tag{6}$$

where $v_1^{=} = \dot{X}\cos\theta_1 + \dot{Y}\sin\theta_1$ is the projection of the velocity of first link along the parallel direction, and $\mu^{=}$ is the drag coefficient. By considering that the cross-sectional area of the other link is much smaller than the first, the flow's effect is reduced and $F_i^{=}(i \geqslant 2)$ is ignored.

Therefore, the composition of forces on the *X*-axis and *Y*-axis are

$$F_x = \sum_{i=1}^{N} F_i^x + F_1^{=} \cos\theta_1, \tag{7}$$

$$F_y = \sum_{i=1}^{N} F_i^y + F_1^{=} \sin\theta_1, \tag{8}$$

where $F_i^x = F_i^{\perp}\sin\theta_i$ and $F_i^y = F_i^{\perp}\cos\theta_i$ are the components of force in the direction of *X*-axis and *Y*-axis, respectively.

The composition of moment acting on the joint point (*X*, *Y*) is

$$M_{\Theta} = \sum_{i=1}^{N} \left[-F_i^x (y_i^{\mathrm{f}} - Y) \right] + \sum_{i=1}^{N} F_i^y (x_i^{\mathrm{f}} - X). \tag{9}$$

Based on eqs. (3) and (7)–(9), a system of partial differential equations of *X*, *Y*, Θ, *t* can be obtained:

$$\begin{cases} F_X = \dfrac{\mathrm{d}}{\mathrm{d}t}\dfrac{\partial L}{\partial \dot{X}} - \dfrac{\partial L}{\partial X} = \displaystyle\sum_{i=1}^{N} F_i^x + F_1^{=}\cos\theta_1, \\ F_Y = \dfrac{\mathrm{d}}{\mathrm{d}t}\dfrac{\partial L}{\partial \dot{Y}} - \dfrac{\partial L}{\partial Y} = \displaystyle\sum_{i=1}^{N} F_i^y + F_1^{=}\sin\theta_1, \\ M_{\Theta} = \dfrac{\mathrm{d}}{\mathrm{d}t}\dfrac{\partial L}{\partial \dot{\Theta}} - \dfrac{\partial L}{\partial \Theta} = \displaystyle\sum_{i=1}^{N} \left[-F_i^x (y_i^{\mathrm{f}} - Y) \right] + \sum_{i=1}^{N} F_i^y (x_i^{\mathrm{f}} - X). \end{cases} \tag{10}$$

The movement of the robotic fish is described by $X(t)$, $Y(t)$, $\Theta(t)$, which are all determined by the tail's motion law $\varphi_i(t)$. The equations are complex, and they are solved by numerical method with boundary conditions at the initial time.

3.2 The yaw control of the robotic fish

While the robotic fish propels itself by undulation of the tail, the orientation of the propulsion can be changed by the symmetric center of undulation. However, the effect of such change is hard to control due to the complicated force. In addition, eq. (10) can be solved numerically, but the analytic solution is hard to obtain. Therefore, the yaw control must be addressed to improve the flexibility and maneuverability of the robotic fish. As a possible way to solve this problem, neural network control methods, which have advantages in controlling complicated plant, are popular in robot control. In this paper, an NN predictive control method is proposed to calculate the undulation law for the robotic fish's yaw control.

As shown in Figure 3, the yaw angle is θ_1, which can be obtained from eq. (10). Then, define the change in the yaw angle as follows:

$$\Delta\theta^n = \theta_1(nT) - \theta_1(nT - T). \tag{11}$$

Eq. (11) is the change in the robotic fish's yaw angle in a period $T=1/f$, which is the undulation period of the tail. The yaw angle can be controlled by the offset δ_i. The neural network control method, which has the ability to learn, can be used in the nonlinear, uncertain, and complicated system, and has advantages in robustness and fault-tolerance. Moreover, the motion model is obtained in Section 3.1, which generates the data to train the NN controller. The NN predictive controller is proposed, and the system diagram is given in Figure 4. The term n_i is the interference noise and n_r is the surge noise. There are two steps in the controller design: the first one is the identification of a neural network plant model, and the second one is the configuration of the controller parameters. The interference noise is the random change in the yaw angle caused by the shock waves or echo waves. The surge noise is caused by stream or ocean currents. This network can be trained offline in a batch mode, using data collected from the plant.

4 The cooperation of MRF & DRF

A specific issue related to the daughter-mother following task is addressed to show the cooperation of the team. The daughter-mother following task requires that DRF firstly swims out the cabin of the MRF, finds and tracks the dynamic light source on MRF, and finally follows the motion of MRF. In this mission, considering the motion in the cooperation, a multiple objective optimization based dynamic

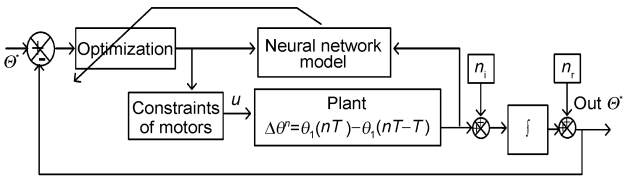

Figure 4 The diagram of the yaw controller.

light source tracking method of the daughter robotic fish is given firstly based on the yaw control of undulation propel.

4.1 The dynamic light source tracking of DRF

Before modeling the task, a multiple objective optimization based dynamic light source tracking method of the daughter robotic fish is given firstly. The inertial frame of reference for the motion is defined as shown in Figure 5, where O is the centre of inertia of the robotic fish, $\vec{r}$ is the direction of the rigid forebody, and γ is angle between $\vec{v}$ and $\vec{r}$.

Three infrared sensors are installed on the robotic fish and their outputs are Boolean variables and labeled as Ir_{l} (left), Ir_{m} (middle), Ir_{r} (right). "1" means there exists an obstacle. The distribution of the sensors is shown in Figure 5. The purpose of avoiding obstacle algorithm is to select the safer direction for the robotic fish. The risk factor function at $t=j$ is defined as follows:

$$\begin{aligned}\mathrm{Risk}_j &= -(Ir_{\mathrm{l},j}\cdot\alpha_{\mathrm{l},j} + Ir_{\mathrm{m},j}\cdot\alpha_{\mathrm{m},j} + Ir_{\mathrm{r},j}\cdot\alpha_{\mathrm{r},j}) \\ &= -[Ir_{\mathrm{l},j}\cdot(90^\circ+\gamma_j) + Ir_{\mathrm{m},j}\cdot|\gamma_j| + Ir_{\mathrm{r},j}\cdot(90^\circ-\gamma_j)]. \quad (12)\end{aligned}$$

The smaller the Risk_j is, the smaller the collision probability of the robotic fish is.

There are seven mini photosensitive sensors installed on the rigid forebody, and the distribution of the sensors is shown in Figure 5.

Label β_j^k as the detecting directions of the kth sensor at $t=j$, as β_j^2 shown in Figure 5. The light intensity detected by the kth sensor is labeled as I_k and the direction of the light source is calculated as follows:

Firstly, if $I_{\max} < I_{\mathrm{env}}$, it means that that is no light source, where $I_{\max}$ is the maximum value of I_k, and I_{env} is the light intensity of environment, else

$$K = \arg \max_{1\leqslant k\leqslant 7}\{I_k\}. \quad (13)$$

Secondly, determine the direction of the light source at $t=j$:

$$\beta_j^* = \sum_{k=K-1}^{k=K+1}(I_k - I_{\mathrm{env}})\cdot\beta_j^k \Big/ \sum_{k=K-1}^{k=K+1}(I_k - I_{\mathrm{env}}). \quad (14)$$

Define the photokinesis function:

$$\mathrm{Light}_j = |\gamma_j - \beta_j^*|. \quad (15)$$

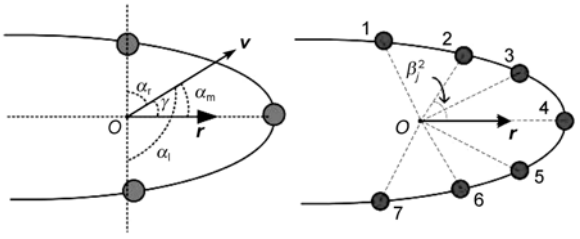

Figure 5 The distribution of infrared/photosensitive sensors.

In an actual task, the robotic fish has to track light source while avoiding obstacles. When the robotic fish is close to the light source, which is both goal and obstacle, the corresponding conflict should be considered. Because of the limited information, the robotic fish can not distinguish the obstacle from the moving light source. Therefore, a multiple objective optimization approach with self-adaptive weight is proposed to solve this problem. The action of the robotic fish is decided by both the infrared sensors and photosensitive sensors:

$$\begin{aligned}\mathrm{Act}_j^* &= \arg \min_{\forall Act_j\in\Phi_{\mathrm{act}}}\{M_1\cdot\mathrm{Light}_j + M_2\cdot\mathrm{Risk}_j\} \\ &= \arg \min_{\forall Act_j\in\Phi_{\mathrm{act}}}\{M_1\cdot|\gamma_j-\beta_j^*| - M_1\cdot[Ir_{\mathrm{l},j}\cdot(90^\circ+\gamma_j) \\ &\quad + Ir_{\mathrm{m},j}\cdot|\gamma_j| + Ir_{\mathrm{r},j}\cdot(90^\circ-\gamma_j)]\}, \quad (16)\end{aligned}$$

where M_1 and M_2 are the weights of the photosensitive and infrared sensors, respectively.

In the light tracking, it can be self-adapted according to the light intensity. When the light is weak, the daughter robotic fish is far from the light source. If an obstacle is detected, the obstacle avoidance should be validated and $M_1 < M_2$ in this case. When the light intensity is high, the obstacle detected may be the light source, thus $M_1 > M_2$. When the light is very high, it means that the robot is very close to the goal, and the obstacle avoiding should be validated to avoid the collision with MRF, therefore we have $M_1 < M_2$.

This decision-making method could fuse multiple sources sensor information and calculate the advance direction. The expected direction can be executed by the yaw controller in Section 3. Based on the yaw control of undulation propel and the decision-making method, the robotic fish can implement the expected motion in the cooperation.

4.2 Task modeling

A cooperation mechanism is necessary for the purpose of team's orderly and effective operation. In this section, a heterogeneous communication-based finite state machine is proposed to model the daughter-mother following task (T_{mcf}). The basic idea is to decompose the task into several states and transit the states according to the information from sensors and communication. It can be described as a quadruple ($\boldsymbol{E}_s$, $\boldsymbol{E}_c$, $\boldsymbol{Q}_s$, σ), and the specification definition are as follows (the symbols with a superscript m or d are related to the mother and the daughter, respectively.):

$\boldsymbol{E}_s = \{e_{s1}^{\mathrm{m}}, e_{s2}^{\mathrm{m}}, \ldots, e_{sl}^{\mathrm{m}}, e_{s1}^{\mathrm{d}}, e_{s2}^{\mathrm{d}}, \ldots, e_{sn}^{\mathrm{d}}\}$: the set of perceptual and internal events.

$\boldsymbol{E}_c = \{e_{c1}^{\mathrm{m}}, e_{c2}^{\mathrm{m}}, \ldots, e_{ck}^{\mathrm{m}}, e_{c1}^{\mathrm{d}}, e_{c2}^{\mathrm{d}}, \ldots, e_{cj}^{\mathrm{d}}\}$: the set of events from the communication.

$\boldsymbol{Q}_s$: the set of discrete states with r+t elements, denoted by $\{q_1^{\mathrm{m}}, q_2^{\mathrm{m}}, \ldots, q_r^{\mathrm{m}}, q_1^{\mathrm{d}}, q_2^{\mathrm{d}}, \ldots, q_t^{\mathrm{d}}\}$.

σ: a mapping from one state to another, expressed by

$\sigma(q_\alpha, \boldsymbol{E}) = q_\beta \in \boldsymbol{Q}_s$, where $q_\alpha \in \boldsymbol{Q}_s$, $\boldsymbol{E} \subset \boldsymbol{E}_s \times \boldsymbol{E}_c$ are the set of perceptual and communication events, respectively.

The initial state of MRF is transporting DRF in the cabin (TRANSP, q_1^{m}), and move together with DRF loaded in (LOADED, q_1^{d}). When the task T_{mcf} starts (Follow, e_{s1}^{m}), MRF stops propelling and opens the cabin (OPEN, q_2^{m}), sends the message "opened" after the cabin is opened. On DRF receiving the message (Opened, e_{s1}^{d}), it starts swimming out of the cabin (FORWARD, q_2^{d}), and sends the message of "out" (OUT, e_{s2}^{d}). DRF then waits (WAIT, q_3^{d}) for next message. MRF closes the cabin (CLOSE, q_3^{m}) after receiving the "out" (Chi_Out, e_{s2}^{m}). MRF opens the controllable light and waits (WAT_LIGH, q_4^{m}) after the cabin is closed (Closed, e_{s3}^{m}), and then sends the message "closed".

On receiving the message of "closed" (Closed, e_{s3}^{d}), DRF starts searching the light source on MRF (SEARCH, q_4^{d}) randomly till it finds the light source (Found, e_{s4}^{d}) according to eq. (16), or else it has not found the light source, according to eq. (16), for a period of time, it sends message "nFound" and keeps searching (Nfound, e_{s5}^{d}). After e_{s4}^{d}, DRF will move to the light source (MOV_LIGH, q_5^{d}) according to eq. (16) with M_1=1 and M_2=0. The state will last if DRF is not near enough to the MRF (Near, e_{s7}^{d}), then DRF will send the message "near", and follow the light source (FOLLOW, q_6^{d}) according to eq. (16). If DRF is far from MRF in following (Far, e_{s6}^{d}), it will send out a message "far", and execute q_5^{d} again to swim toward MRF. DRF may lost the light signal (MLost, e_{s8}^{d} /FLost, e_{s9}^{d}) in the process of moving toward/following the light source. In this case, it will send the message of "mLost"/"fLost" and execute searching the light source randomly again.

MRF on the state of waiting (q_4^{m}) will adjust its position (ADJUST, q_5^{m}) when it gets the message of "nFound" or "mLost" (Chi_Lost, e_{c2}^{m}). q_5^{m} is that MRF propels and turns with a slight motion to adjust the position of MRF a little, and switches back q_4^{m} after the motion is finished (Adjust_OK, e_{s4}^{m}). If MRF receives "near" (Chi_Neat, e_{c6}^{m}), which means it confirms to establish the connection with DRF, it will advance slowly (equal to the max velocity of DRF approximately) to maintain the relative position (WAT_LIGH, q_6^{m}). MRF will execute q_4^{m} immediately if it receives the message of "far" (Chi_FarFL, e_{c5}^{m}), which means the DRF is far from MRF, and so it is when it receives the message "fLost" (Chi_Lost, e_{c7}^{m}), which means DRF loses the light signal suddenly when following.

Based on the above description, the model of the daughter-mother following task is shown in Figure 6. The possible state transitions are as follows.

MRF: $\sigma(q_1^{\mathrm{m}}, e_{s1}^{\mathrm{m}}) = q_2^{\mathrm{m}}$, $\sigma(q_2^{\mathrm{m}}, e_{s2}^{\mathrm{m}}) = q_3^{\mathrm{m}}$, $\sigma(q_3^{\mathrm{m}}, e_{s3}^{\mathrm{m}}) = q_4^{\mathrm{m}}$, $\sigma(q_4^{\mathrm{m}}, e_s^{\mathrm{m}}) = q_6^{\mathrm{m}}$, $\sigma(q_6^{\mathrm{m}}, e_{c5}^{\mathrm{m}}) = q_4^{\mathrm{m}}$, $\sigma(q_4^{\mathrm{m}}, e_{c7}^{\mathrm{m}}) = q_5^{\mathrm{m}}$, $\sigma(q_5^{\mathrm{m}}, e_{s4}^{\mathrm{m}}) = q_4^{\mathrm{m}}$.

D R F: $\sigma(q_1^{\mathrm{d}}, e_{s1}^{\mathrm{d}}) = q_2^{\mathrm{d}}$, $\sigma(q_2^{\mathrm{d}}, e_{s2}^{\mathrm{d}}) = q_3^{\mathrm{d}}$, $\sigma(q_3^{\mathrm{d}}, e_{s3}^{\mathrm{d}}) = q_4^{\mathrm{d}}$,

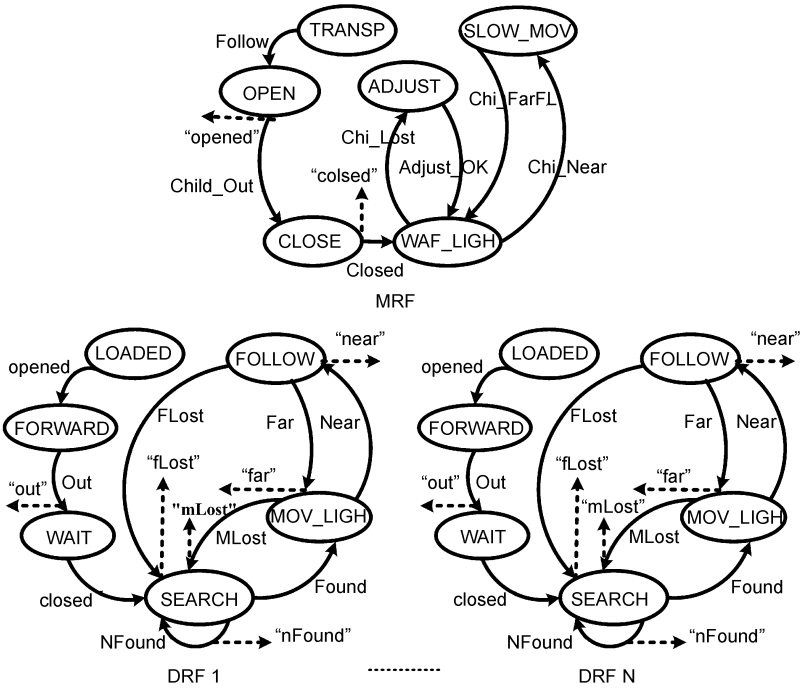

Figure 6 The model of daughter-mother following task.

$\sigma(q_4^{\mathrm{d}}, e_{s5}^{\mathrm{d}}) = q_4^{\mathrm{d}}$, $\sigma(q_4^{\mathrm{d}}, e_{s5}^{\mathrm{d}}) = q_5^{\mathrm{d}}$, $\sigma(q_5^{\mathrm{d}}, e_{s7}^{\mathrm{d}}) = q_6^{\mathrm{d}}$, $\sigma(q_6^{\mathrm{d}}, e_{s6}^{\mathrm{d}}) = q_5^{\mathrm{d}}$, $\sigma(q_6^{\mathrm{d}}, e_{s9}^{\mathrm{d}}) = q_4^{\mathrm{d}}$, $\sigma(q_1^{\mathrm{d}}, e_{s8}^{\mathrm{d}}) = q_4^{\mathrm{d}}$.

5 Experiments

The developed robotic fish prototypes are shown in Figure 7.

Figure 8 gives the simulation and experiment results of DRF with $A_1=\pi/4$, $f=2.14$ Hz. The head of robotic fish is assumed to point to the negative direction of X axis, and the position is at the origin point at the initial time. Eq. (10) is solved to obtain $X(t)$, $Y(t)$, $\Theta(t)$. It is shown that the orientation is not the direction that the robotic fish pointed to at the initial time. It is because that forces acting on robotic fish are not symmetrical when it starts. The experimental track is not on a line because the installation error. The installation error is that the tail is not strictly mounted in the middle, which makes the undulation not symmetrical a little.

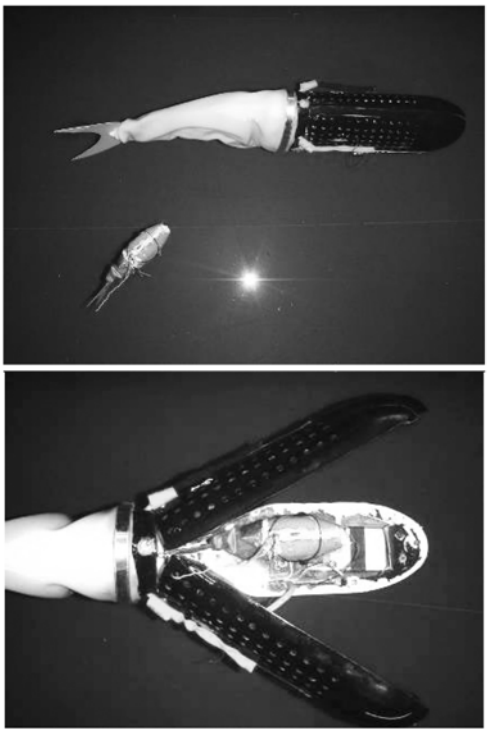

Figure 7 The prototypes of robotic fish MRF and DRF.

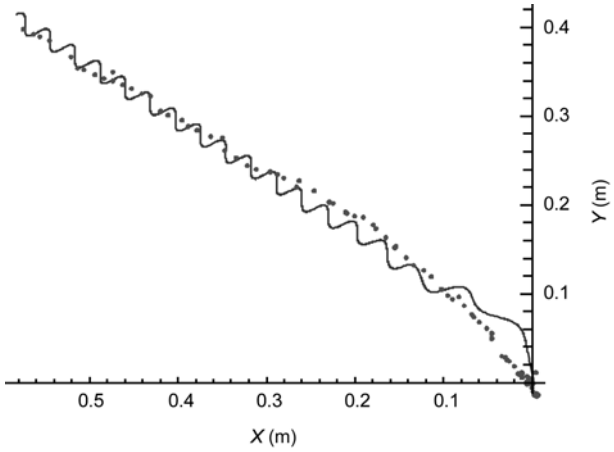

Figure 8 Simulated and experimental data of forward motion (Simulated data is shown in solid line, and experimental data in dots).

The turning motion of DRF is simulated with $A_1=\pi/5$, $f=2.50$ Hz, and $\delta_i=\pi/18$. Figure 9 gives the simulated and experimental results of the turning. The average turning radius R is 0.196 m, the average velocity 0.0604 m/s and the average angular velocity 0.309 rad/s.

Figure 10 gives the simulated results with the interference noise and the surge noise. The noise is white noise with zero mean and variance of $\pi/3600$. The expectation of the error in Figure 10 is $E=4.38\times10^{-3}$ and the variance of the error $D=2.31\times10^{-2}$.

Based on the proposed HCFSM, the daughter-mother following task is performed. Figure 11 shows a motion sequence of the marsupial robotic fish swimming in the experiment pool. Figure 12 shows the corresponding motion

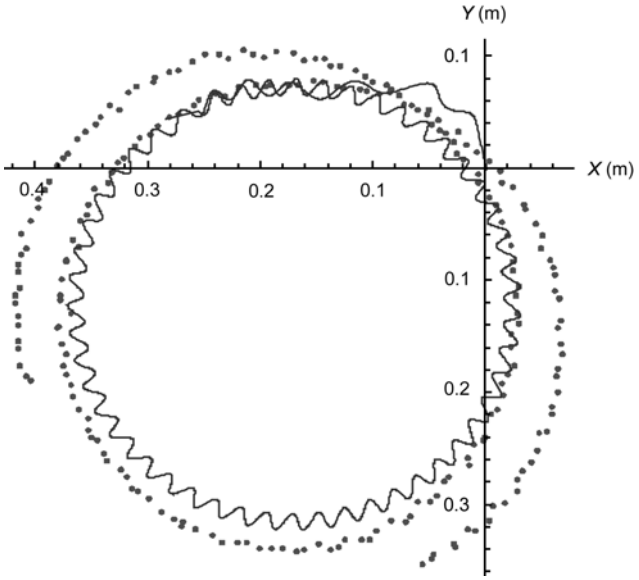

Figure 9 Simulated and experimental data of turning motion (Simulated data is shown solid line, and experimental data in dots).

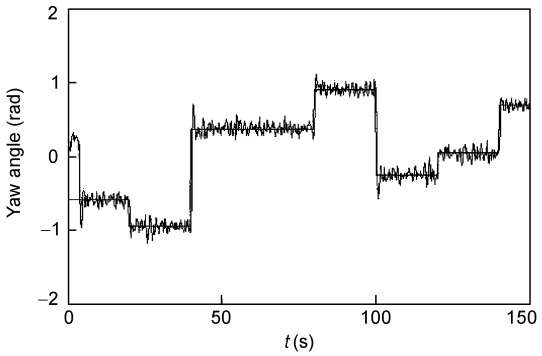

Figure 10 The simulated response to a random change step signal with the interference noise.

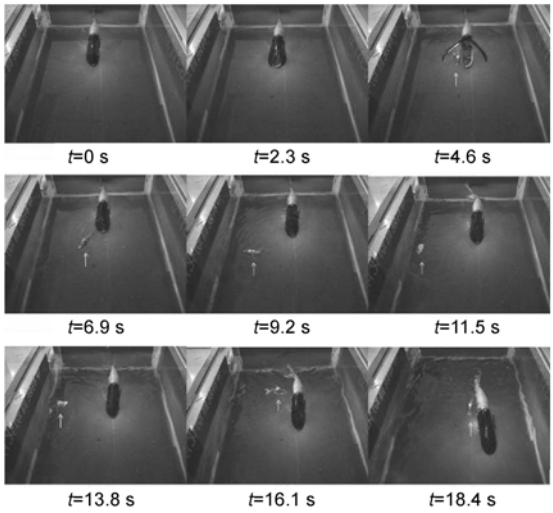

Figure 11 Selected images of the motions.

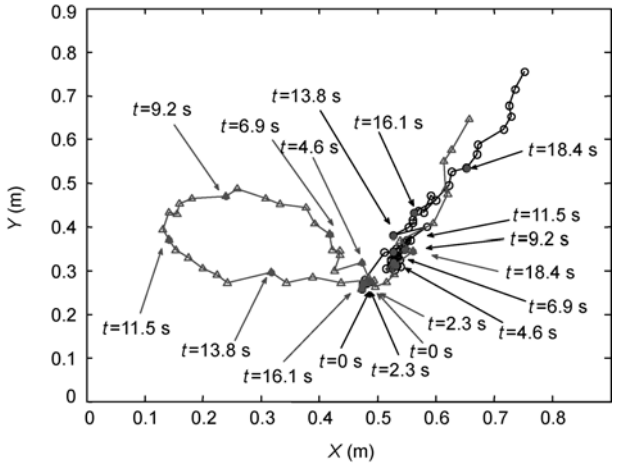

Figure 12 The trajectories of motions (The dot is the track of MRF, and the triangle is the track of DRF).

trajectories, which shows the effectiveness of the team.

6 Conclusions

In this paper, a marsupial robotic fish team composed of a mother robotic fish with a cabin and a daughter robotic fish is designed based on fish-like motion. In order to decouple the dynamic and kinematic functions, which can eliminate effects of the head's oscillation, the motion of the robotic fish is described by the equality relation between the generalized force and fluid force. An NN predictive yaw controller is designed to change the offset of links, which can control the orientation. A typical cooperative daughter-mother following task is modeled based on a heterogeneous communication-based finite state machine. Experiments have verified the design and method of the team. As a new concept of robotic fish prototype, the marsupial robotic fish may be used in many special situations.

This work was supported in part by the National Natural Science Foundation of China (Grant Nos. 60805038, 60725309, 60635010).

1 Triantafyllou M S, Triantafyllou G S. An efficient swimming machine. Sci Am, 1995, 272(3): 64–70
2 Sfakiotakis M, Lane D M, Davies J B C. Review of fish swimming modes for aquatic locomotion. IEEE J Ocean Eng, 1999, 24(2): 237–252
3 Terada Y, Yamamoto I. An animatronic system including lifelike robotic fish. Proc IEEE, 2004, 92(11): 1814–1820
4 Barret D S, Triantafyllou M S, Yue D K P, et al. Drag reduction in fish-like locomotion. J Fluid Mech, 1999, 392: 183–212
5 Kato N. Pectoral Fin Controllers: Neurotechnology for Biometric Robots. Cambridge: MIT Press, 2002. 325–350
6 Kato N. Control performance in the horizontal plane of a fish robot with mechanical pectoral fins. IEEE J Ocean Eng, 2000, 25(1): 121–129
7 Fukuda T, Kawamoto A, Arai F, et al. Mechnism and swimming experiment of micro mobile robot in water. In: Proceedings of IEEE Workshop on Micro Electro Mechanical Systems, 1994, Kyoto, Japan
8 Liu J, Hu H. Building a 3D simulator for autonomous navigation of robotic fishes. In: Proceedings of International Conference on Intelligent Robots and Systems, 2004, Sendai, Japan
9 Low K H, Willy A. Biomimetic motion planning of an undulating robotic fish fin. J Vib Contr, 2006, 12(12): 1337–1359
10 Zhou C, Nahavandi S, Gu N, et al. Analysis and implementation of swimming backward for biomimetic Carangiform robot fish. In: Proceedings of the 17th World Congress of The International Federation of Automatic Control, 2008, Coex, Korea
11 Zhou C, Cao Z, Wang S, et al. A marsupial robotic fish system. In: Proceedings of the 17th World Congress of The International Federation of Automatic Control, 2008, Coex, Korea
12 Murphy R R. Marsupial robots for urban search and rescue. Proc IEEE Intell Syst, 2000, 2: 14–19
13 Minten B, Murphy R, Hyams J, et al. Low order complexity vision-based docking. IEEE T Robot Auto, 2001, 17(6): 922–930
14 Breder C M. The locomotion of fishes. Zoologica, 1926, 4: 159–256
15 Vela A, Burdick J W. Trajectory stabilization for a planar Carangiform robot fish. In: Proceedings of IEEE International Conference on Robotics and Automation, 2002, Washington, USA
16 Morgansen K A, Triplett B I, Klein D J. Geometric methods for modeling and control of free-swimming fin-actuated underwater vehicles. IEEE T Robot, 2007, (6): 1184–1199
17 Wu T Y. Swimming of a waving plate. J Fluid Mech, 1961, 10(3): 321–344
18 Ayers J, Rulkov N. Controlling Biomimetic Underwater Robots with Electronic Nervous Systems: Bio-mechanisms of Animals in Swimming and Flying. Berlin: Springer-Verlag, 2008. 295–306